ISSN 1027-4510, Journal of Surface Investigation: X-ray, Synchrotron and Neutron Techniques, 2017, Vol. 11, No. 3, pp. 585–589. © Pleiades Publishing, Ltd., 2017.
Original Russian Text © S.E. Kichanov, K.M. Nazarov, D.P. Kozlenko, I.A. Saprykina, E.V. Lukin, B.N. Savenko, 2017, published in Poverkhnost', 2017, No. 6, pp. 11–15.

# Analysis of the Internal Structure of Ancient Copper Coins by Neutron Tomography

**S. E. Kichanov[a], *, K. M. Nazarov[a, b], **, D. P. Kozlenko[a], ***, I. A. Saprykina[c], E. V. Lukin[a], and B. N. Savenko[a]**

[a]*Joint Institute for Nuclear Research, Dubna, Moscow oblast, 141980 Russia*
[b]*Dubna University, Dubna, Moscow oblast, 141980 Russia*
[c]*Institute of Archeology, Russian Academy of Sciences, Moscow 117036 Russia*
**e-mail: ekich@nf.jinr.ru*
***e-mail: quanysh@list.ru*
****e-mail: denk@nf.jinr.ru*
Received September 23, 2016

**Abstract**—The internal structure of copper coins—a Golden Horde pulo of the 14th century AD and an ancient coin found in Phanagoria at sites of the 5–4th centuries BC—are studied by neutron tomography method. From a set of angular projections of neutron absorption, three-dimensional models of the analyzed objects are reconstructed and the analysis of their physical state is performed. In the copper pulo, a region characterized by a greater neutron beam attenuation coefficient is found. It is assumed that this region was formed due to the gradual penetration of patina into the coin. The neutron tomography data also make it possible to analyze the remnants of an antique coin found in underwater archeological studies. Areas of surface damage and cracks in the antique coin are shown, visually separated from the corrosion layer.

*Keywords:* neutron radiography and tomography, Golden Horde pulo, antique coin, three-dimensional model, corrosion, patina layer on a coin surface

**DOI:** 10.1134/S1027451017030296

## INTRODUCTION

One of the important lines of research concerning the conservation of cultural heritage, archeology and history involves determining the degree of degradation of objects: recording of losses, revealing surface and internal defects, analysis of variations in the chemical and phase compositions, study of the structural features of objects, and simulation of the development of corrosion processes [1, 2]. Archeological objects and objects of cultural heritage are valuable due to their uniqueness and antiquity; therefore, it is desirable to study them by modern non-destructive methods [3]. One such method giving sufficiently complete information on the surface and the internal structure of analyzed objects is neutron radiography and tomography method [3–6]. The difference in the neutron absorption cross section for different elements makes it possible to visualize the distribution of composition and structural irregularities in objects and materials and obtain their three-dimensional models for further analysis [4, 5, 7]. Neutron radiography and tomography are often used to study archeological objects, especially metallic artifacts [3, 8, 9]. This is connected with the high X-ray absorption in materials containing heavy-elements, which imposes restrictions on the use of X-ray radiography and tomography in the analysis of solid metallic objects [7]. In particular, neutron radiography was used for the analysis of bronze objects of the Roman period: the figure of a dog and a solid lamp [8, 9], arms from medieval Europe and Japan [3, 10], and lead sculptures of the early modern period [11]. From the results of these studies, the technology of the analyzed objects was reconstructed and corroded areas and changes in the internal structure of the material were determined. Separate elements inside analyzed objects: ash in a sealed urn [12] and a support rod in a bronze figure of Buddha [15] were successfully visualized [13].

One of the most promising objects for neutron radiography and tomography are coins, which are valuable objects for museum exhibition and are an important source for historical reconstructions. In addition, coins are convenient model objects [14] to study corrosion processes on the surface of copper, bronze, silver, and gold archeological finds, which is important for the development of methods of restoration and conservation of valuable archeological finds.

In this work, we present the results of analysis of the distribution of internal irregularities inside ancient

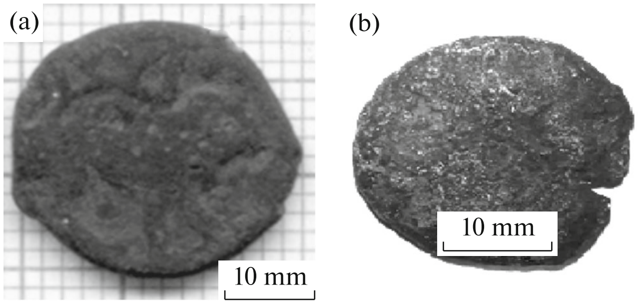


**Fig. 1.** Copper coins under study: (a) a Golden Horde pulo and (b) an antique coin.

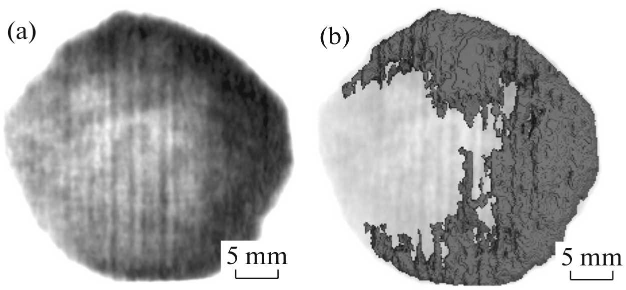


**Fig. 2.** 3D models of the copper pulo: (a) the model reconstructed from neutron tomography data (light regions correspond to minimum attenuation of the neutron beam and dark regions are characterized by a large total neutron-beam absorption cross sections) and (b) the model with a highlighted crescent-shaped region with high neutron beam absorption coefficients.

copper coins by neutron tomography. The first analyzed coin is a copper pulo dated to be from the reign of Uzbek-Khan (Golden Horde) [15, 16]. The main purpose of the analysis of this coin is to record the corrosion processes in classical copper archeological objects. The second object of neutron analysis is an antique copper coin that was found during underwater archeological studies in the port zone of the ancient polis of Phanagoria, situated on the shore of Taman bay. The antique coin is enclosed in a thick layer of blue–green corrosion products mixed with silt bottom sediments. The neutron tomography data make it possible to obtain a volumetric three-dimensional image of the remnants of the coin inside this specific surface layer. The results of this study are important for reconstruction of the decay of antique copper objects under the action of aggressive salt water environment and for a fundamental understanding of the processes of the decay of copper and bronze objects under the surface layer of corrosion products.

## 1. EXPERIMENTAL

Figure 1 shows the studied archeological objects: a copper pulo and an antique copper coin. The Golden Horde copper pulo (Fig. 1a) is dated to be from 1336–1342 AD, the reign of Uzbek-Khan, when the economic and political center of the Golden Horde moved from Bulgar to the new capital Sarai [15, 16]. In this period, money reform was performed, when an exchange rate between copper pulos and silver dangas was established [15, 16]. On the averse of this coin, a lion with the sun ascending behind is depicted, and the reverse has an inscription "pulo" in Turkic [16].

The antique coin (Fig. 1b) was found during underwater studies in 2015 in the coastal (port) zone of ancient Phanagoria, site "Staroe dno" [16, 17]. The copper coin is covered with a blue–green corrosion layer mixed with silt bottom deposits. As a rule, this type of corrosion, which has an unstable system, appears under the action of sea water with the release of carbon dioxide. The unstable system of this type of corrosion facilitates the emergence of cuprite ($Cu_2O$) on the surface with subsequent total destruction of the sample [18].

The neutron study of the coins was performed on a specialized radiography and tomography station [19, 20] at the 14th beamline of the IBR-2 pulse high flux reactor. Due to the different attenuation of a neutron flux [21] upon passage through components of different chemical compositions and densities, one can obtain information on the internal structure of analyzed materials with micrometer spatial resolution [2, 4]. A neutron beam with a cross section of $20 \times 20$ cm$^2$ was formed by a collimator system with a characteristic parameter $L/D$ of 200 ($L$ is the distance between the input aperture of the collimator system and the position of the sample and $D$ is the diameter of the input aperture of the collimator system) [22]. The integrated flux of thermal neutrons, $\Phi$, at the sample was ~5.5(2) $\times$ $10^6$ n/cm$^2$/s. Neutron diffraction patterns of the coins were obtained by means of a detector system on the basis of a $^6$LiF/ZnS scintillation screen with the detection of images by a highly sensitive CCD video camera. The tomography experiments were carried out with a HUBER goniometer system with a minimum rotation angle of 0.02°. The experimental neutron images were corrected with allowance for the background noise of the detector system and normalized to the incident neutron flux with the help of the ImageJ software package [23]. The tomographic reconstruction of angular neutron projections of the analyzed coins was performed by means of the H-PITRE code [24]. For visualization and analysis of the obtained 3D data, the VGStudio MAX 2.2 (Volume Graphics, Heidelberg, Germany) program complex was used.


**Fig. 3.** Virtual cross section of the copper pulo from the analysis of a 3D model. Dark areas correspond to regions with greater neutron-beam attenuation coefficients and, presumably, are associated with patina. Lighter areas correspond to copper.

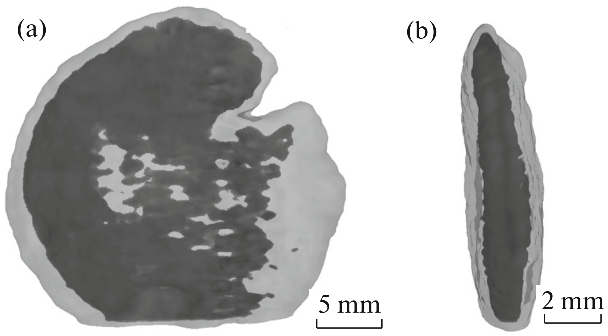


**Fig. 4.** 3D model of the antique coin reconstructed from neutron tomography data: (a) the model (light regions correspond to minimum attenuation of the neutron beam and correspond to the sand and silt crust on the surface of the coin) and (b) the virtual slice of the model (dark areas correspond to copper remnants of the coin and light areas, to the silt and sand crust).

## 2. RESULTS AND DISCUSSION

### *2.1. Neutron Analysis of the Golden Horde copper pulo*

The internal structure of the copper pulo was studied in a series of radiographic experiments, in which a set of 360 angular projections of the analyzed coin was obtained. From the set of radiographic projections, a 3D model of the given pulo was reconstructed (Fig. 2). This 3D model comprises an array of 3D pixels (voxels), each characterized by spatial coordinates and a certain value of grayscale [25]. The size of one voxel in the reconstructed tomographic data was 53 × 53 × 53 $\mu m^3$. The grayscale reflects the degree of attenuation of the neutron beam at a certain sample point and ranges from 0 arbitrary units (arb. units), which corresponds to a medium fully transparent to neutrons, to 65536 arb. units, which corresponds to maximum neutron absorption.

It is seen from Fig. 2a that the neutron-beam attenuation inside the analyzed coin is anisotropic. The middle part of the coin attenuates the neutron beam insignificantly while, near the edge, there is a large crescent-shaped region characterized by a higher total neutron absorption cross section.

From the 3D tomographic data obtained, a region [26] with higher neutron absorption was virtually separated (Fig. 2b). Knowing the parameter of one voxel, it is easy to calculate the volume occupied by the region. In particular, the entire volume of the analyzed coin is formed by 10580375 voxels, which corresponds to 1575.17 $mm^3$. The separated region consists of 1004822 voxels and has a volume of 149.59(1) $mm^3$, which comprises 9.47% of the entire volume of the coin.

Figure 3 shows a virtual slice of the copper pulo. Regions characterized by higher neutron-beam attenuation are localized on one side of the coin, which determined the crescent shape of the irregularity. In addition, a thin surface layer characterized by a high total neutron absorption cross section is observed. The mean thickness of this layer is about 300 μm.

The difference in the neutron-beam attenuation coefficient in the volume of the copper pulo can be explained by changes in the structure and chemical composition of the metal of the coin with time. It is known [27] that, on the surface of copper coins, a patina layer, characterized by a high content of copper oxides or sulfites, is formed. The color of the coin indicates the dominance of a simple copper oxide

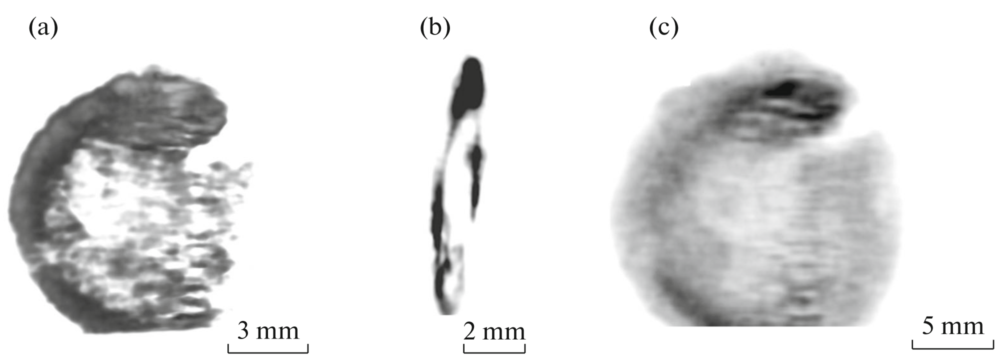


**Fig. 5.** 3D model of the remnants of the antique coin reconstructed from neutron tomography data: (a) the model, (b) the slice of the model (dark areas correspond to copper or copper-containing zones inside the coin), and (c) virtual longitudinal section of the model (dark areas correspond to copper remnants of the coin).

CuO in the patina layer of the coin. From the results obtained, it follows that a corrosion layer in the sample under study is formed on the surface and zones of its penetration into the bulk of the sample correspond to microcracks and fractures in the coin. A rough estimate of the patina penetration rate into the coin is 1 volume percent per 70 years.

### *2.2. Analysis of the Antique Coin by Neutron Tomography*

The model of the antique coin obtained after reconstructing three-dimensional neutron tomography data from a series of angular projections is presented in Fig. 4. The differences in the neutron-beam attenuation coefficient [21] of silicates and different salts, which mainly form the surface deposit on the coin, and copper causes a strong radiographic contrast between these components. It is seen that the antique coin is greatly damaged and only a narrow crescent-shaped edge of the original coin remains. From the tomography data obtained, a 3D model of the remnants of the coin was extracted (Fig. 5a). The entire volume of the analyzed archeological object is 1082.82(1) $mm^3$, while the remnants of the antique coin have a volume of 250.90(3) $mm^3$. The thickness of the silt and sand layer around the coin falls into the range of 800–1100 μm.

Besides the crescent-shaped edge of the coin, thin copper or copper-containing layers remain on the averse and reverse of the coin. These thin layers are distinctly seen in the cross sections of the tomography model of the coin (Fig. 5b). The thickness of these layers does not exceed 300–500 μm.

Figure 5c shows a vertical slice of the analyzed coin. A crescent-shaped copper edge is distinctly seen, and the middle part of the coin is totally destroyed. Sea water penetrates into the coin through a deep lateral crack (Fig. 5b). It is seen in the figure that the base of the coin is a corrosion layer, replacing metal (copper or bronze) almost completely, which gives us insight into the processes occurring in ancient metal under the action of sea water.

From neutron tomography data on the preserved copper edge, we can calculate the diameter of the copper coin exactly: 19.9 mm. The maximum thickness of the crescent-shaped edge of the coin is 1.97 mm. Then, knowing the density of copper, we can estimate the mass of the antique coin analyzed to be 5.6 g.

## CONCLUSIONS

Irregularities and their spatial distribution in the bulk of two ancient coins: a copper pulo and an antique coin from the site "Staroe dno", dated to be from the 5th–4th centuries BC, have been studied by neutron tomography. The specifics of the interaction of neutrons with different substances made it possible to estimate and analyze irregularities on the surface and inside the copper pulo, possibly connected with patina penetration into the bulk of the copper coin. In addition, with the help of neutron tomography, remnants of the ancient coin covered with a corrison layer mixed with bottom sediments have been studied in detail. It has been established that, presently, the coin is an almost completely lost object with small preserved regions inside the corrosion layer. At the same time, no emergence of cuprite ($Cu_2O$) on the surface of the analyzed object has been detected, which evidences a certain stability of the system and the possibility of using the coin in its preserved form for exhibition.

## ACKNOWLEDGMENTS

We are grateful to V.D. Kuznetsov and S.V. Ol'khovskii, leaders of archeological works in 2015 at the underwater site "Staroe dno" in the coastal zone of Phanagoria, for providing us with the coins for the study.

## REFERENCES

1. *Non-Destructive Micro Analysis of Cultural Heritage Materials,* Ed. by K. Janssens and R. Van Grieken (Elsevier Science, 2005).
2. A. Middleton, J. Tum, and J. Lang, *Radiography of Cultural Material* (Routledge, London, New York, 2005).
3. D. Mannes, F. Schmid, J. Frey, K. Schmidt-Ott, and E. Lehmann, Phys. Procedia **69**, 653 (2015).
4. *Neutron Imaging and Applications: A Reference for the Imaging Community,* Ed. by I. S. Anderson, R. L. McGreevy, and H. Z. Bilheux (Springer, New York, 2009).
5. T. Mongy, Appl. Radiat. Isot. **85**, 54 (2014).
6. A. A. Kaloyan, E. S. Kovalenko, A. V. Pakhnevich, K. M. Podurets, S. V. Rozhnov, and V. A. Somenkov, J. Surf. Invest.: X-ray, Synchrotron Neutron Tech. **8** (6), 1093 (2014).
7. A. V. Belushkin, D. P. Kozlenko, and A. V. Rogachev, J. Surf. Invest.: X-ray, Synchrotron Neutron Tech. **5** (5), 828 (2011).
8. E. H. Lehmann, E. Deschler-Erb, and A. Ford, Archaeometry **52**, 272 (2010).
9. K. Ryzewski, S. Herringer, H. Bilheux, L. Walker, B. Sheldon, S. Voisin, J.-C. Bilheux, and V. Finocchiaro, Phys. Procedia **43**, 343 (2013).
10. F. Salvemini, F. Grazzi, A. Fedrigo, A. Williams, F. Civita, A. Scherillo, and P. Vontobe, Eur. Phys. J. Plus **128**, 87 (2013).
11. D. Mannes, E. Lehmann, A. Masalles, K. Schmidt-Ott, A. V. Przychowski, K. Schaeppi, F. Schmid, and S. Peeterman, Insight (Northampton, U. K.) **56** (3), 137 (2014).
12. L. Harvig, N. Lynnerup, and J. Ebsen, Archaeometry **54**, 369 (2012).
13. E. H. Lehmann, S. Hartmann, and M. O. Speidel, Archaeometry **52**, 416 (2010).

14. M. Griesser, R. Traum, K. Vondrovec, P. Vontobel, and E. Lehmann, IOP Conf. Ser.: Mater. Sci. Eng. **37** (1), 899 (2012).

15. A. G. Mukhamadiev, *Bulgaro-Tatarian Coinage System, 12–15 Centuries* (Nauka, Moscow, 1983) [in Russian].

16. M. O. Zhukovsky, V. D. Kuznetsov, and S. V. Olkhovsky, in *Proc. 24th Int. CIPA Symposium* (Strasbourg, 2013), Vol. 40-5, p. 717.

17. V. D. Kuznetsov, Am. J. Archaeol. **113** (2), 104 (2009).

18. D. A. Scott, *Copper and Bronze in Art: Corrosion, Colorants, Conservation* (Getty Conservation Institute, Los Angeles, 2002).

19. D. P. Kozlenko, S. E. Kichanov, E. V. Lukin, A. V. Rutkauskas, A. V. Belushkin, G. D. Bokuchava, and B. N. Savenko, Phys. Part. Nucl. Lett. **13**, 346 (2016).

20. D. P. Kozlenko, S. E. Kichanov, E. V. Lukin, A. V. Rutkauskas, G. D. Bokuchava, B. N. Savenko, A. V. Pakhnevich, and A. Yu. Rozanov, Phys. Procedia **69**, 87 (2015).

21. V. F. Searf, Neutron News **3** (3), 29 (1992).

22. M. Dinca and M. Pavelescu, Rom. J. Phys. **51** (3–4), 435 (2006).

23. C. A. Schneider, W. S. Rasband, and K. W. Eliceiri, Nat. Methods **9** (7), 671 (2012).

24. R. C. Chen, D. Dreossi, L. Mancini, R. Menk, L. Rigon, T. Q. Xiao, and R. Longo, J. Synchrotron Radiat. **19**, 836 (2012).

25. E. H. Lehmann, A. Kaestner, C. Gruenzweig, D. Mannes, P. Vontobel, and S. Peetermans, Int. J. Mater. Res. **105**, 664 (2014).

26. J. Ollion, J. Cochennec, F. Loll, C. Escudé, and T. Boudier, Bioinformatics **29** (14), 1840 (2013).

27. K. P. Fitzgerald, J. Nairn, and A. Atrens, Corros. Sci. **40** (12), 2029 (1998).

*Translated by E. Chernokozhin*